Fluid-Structure Interaction involving Close-in Detonation Effects on Column using LBE MM-ALE Method

Swee Hong TAN, Shih Kwang TAY, Jiing Koon POON and David CHNG

Ministry of Home Affairs, Singapore

Abstract

*This paper shares the experiences gathered from studies conducted on the use of *Load_Blast_Enhanced (LBE) keyword to couple empirical blast loads to air domain in Multi-Material Arbitrary Lagrangian-Euler (MM-ALE) environment and on Fluid-Structure Interaction (FSI) computations relating to various aspects of coupling technique in LS-DYNA® via *Constrained_Lagrange_in_Solid keyword for structures composing of mainly solid elements.*

This paper also presents a case-study in which results from the LBE MM-ALE FSI simulation were compared to experimental data from full-scale blast trials, as well as results from associated pre-test simulations. The pre-test simulations were done using a 2-stage numerical approach which involved applying segmental pressure loadings derived from Computational Fluid Dynamics (CFD) calculations on LS-DYNA Lagrangian models to predict structural response.

1. Introduction

The *Load_Blast_Enhanced (LBE) keyword implemented in LS-DYNA since 2009 offers more features over its predecessor, *Load_Blast keyword [1]. The improved version allows consideration of two more blast sources, namely air burst due to moving non-spherical warhead and air burst with ground reflection which is commonly known as the Mach Stem phenomenon. These are in addition to hemispherical surface burst and spherical air bursts originally found in *Load_Blast keyword.

Another significant inclusion is its latest capability to couple empirical blast loads to air domain in Multi-Material Arbitrary Lagrangian-Euler (MM-ALE) environment. Not only it means that Fluid-Structure Interaction (FSI) calculations can be carried out in tandem with LBE, the clear advantage of adopting the method is that it can allow upfront reduction of computational costs due to a smaller air space required as compared to a MM-ALE approach.

The theoretical fundamentals behind the empirical blasts models were briefly explained by Todd P. Slavik [2] from Livermore Software Technology Corporation (LSTC). He used experimental data as the basis for comparison of three key air blast simulation techniques, namely the LBE MM-ALE, MM-ALE and Empirical, showcasing the validity as well as the benefits of using the new method. Len Schwer [3] offered his perspective on the LBE MM-ALE coupling method for air blast propagation calculations. He provided a schematic illustration in an easy-to-understand manner on how computational size can be reduced drastically in relation to a MM-ALE approach. Using a simple plane strain model, he demonstrated in details, the effects of expansion waves from boundaries and stressed the importance of having sufficient MM-ALE domain in order to avoid such effects reducing the accuracy at the region of interest.

Ministry of Home Affairs, Singapore (MHA) had shared the comparisons of some pre-test simulation results against the experimental findings from full-scale blast trials, which were conducted as part of a long-term technology development programme to study close-in, contact and near contact blast effects on structural elements as well as the mechanism of progressive collapse [4]. Those pre-test simulations were carried out via a 2-stage numerical approach which involved applying segmental pressure loadings derived from Computational Fluid Dynamics (CFD) calculations on LS-DYNA Lagrangian models to predict structural response. Reasonable comparisons were achieved and useful insights were gained. MHA went on to investigate and assess the use of LBE MM-ALE coupling method in tandem with FSI as an alternative to the previous CFD-Lagrangian approach.

This paper shares the experiences gathered on separate studies conducted on LBE MM-ALE and FSI and lastly, presents a case-study in which results from the LBE MM-ALE FSI simulation were compared to the results from earlier pre-test computations using the CFD-Lagrangian approach and associated field measurements. The work discussed in this paper is not meant to be a full illustration of verification and validation procedures [5,6]. Simulation runs were planned to the best resolution that existing in-house computational capability could offer so as to test the various aspects of related techniques in a calibrated way.

2. LBE MM-ALE

To counter the adverse effects of expansion waves from boundaries, a sizable air domain is needed. While the proposition behind LBE MM-ALE coupling method points to a smaller computational size and has made air blast propagation calculations more affordable, the requirement to address boundaries' effects remains. This is on top of the general rule that mesh size of air elements has to be fine enough to ensure integrity of results.

One question that arises is whether accuracy can be attainable by a typical single workstation running on Shared Memory Parallel Processing (SMP) mode, as opposed to a cluster of machines on Massively Parallel Processing (MPP) which is typical for MM-ALE problems. Another question is whether there are additional considerations to look out for in relation to LBE MM-ALE specifically.

It is pertinent to note that the advection loss in LBE MM-ALE cases cannot be accounted for via the current total energy (hence also the energy ratio, that monitors the proportion of current total energy versus initial total energy), as opposed to MM-ALE cases. Once empirical blast load reaches the receptor air layer, current total energy increases sharply and goes into oscillation, as seen from Figure 1. It is unclear how to interpret such plots.

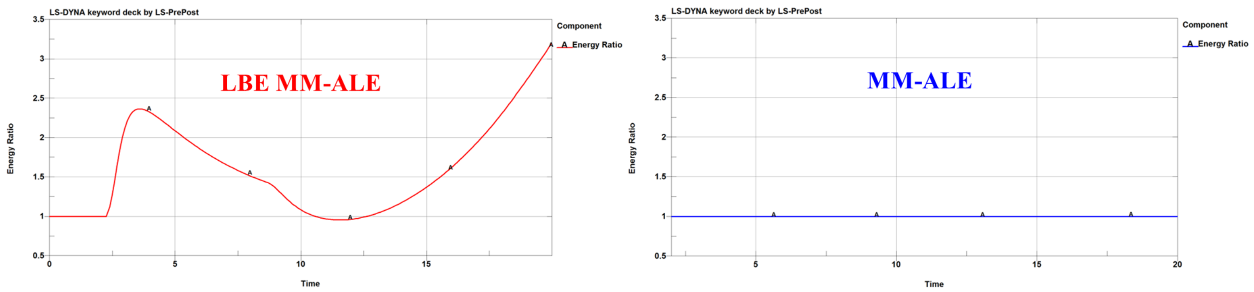

Figure 1: Typical Energy Ratio Plots of LBE MM-ALE & MM-ALE

An indirect way of checking whether advection loss has affected air blast propagation computations is to track and compare key outputs from pressure time histories in specific locations of air domains against known solutions from established charts such as UFC 3-340-02 [7] and equations from related literature.

Figure 2 shows the four air configurations created to assess the ability of LBE MM-ALE coupling method to calculate air blast propagation. Maximum number of air elements used was 8 million cells, which is approximately the limit that existing in-house computational capability can offer based on a separate in-house study. Current workstation is running on Intel® Core™ i7 870 @ 2.93 GHz with 16.0 GB installed memory on four LS-DYNA SMP licenses.

Air Configuration 1 and 2 consisted of air elements of regular mesh sizes, 33.33 mm and 25 mm respectively. Air Configuration 3 and 4 were built up by air elements of irregular mesh sizes, involving smallest mesh size at 10 mm and 5 mm in zones that measured 3000 mm by 500 mm by 500 mm, as seen from Figure 3. Pressure time histories were tracked at six locations; the first in the ambient air element in the receptor layer till the sixth located 400 mm from the edge of receptor layer.

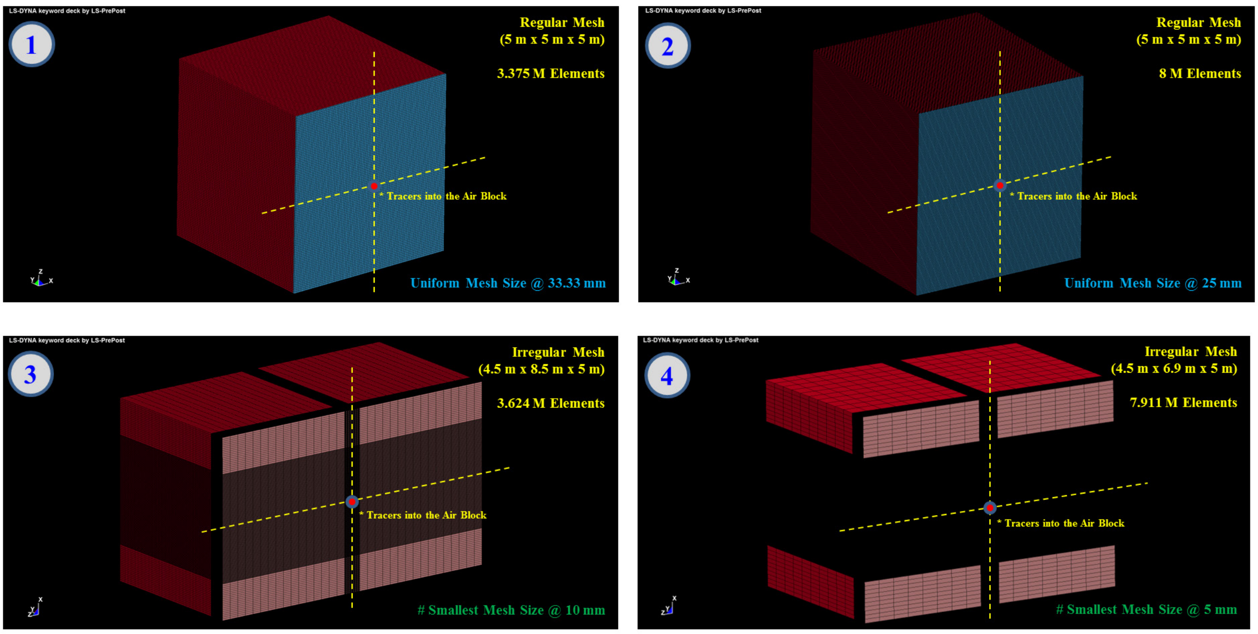

Figure 2: Four Air Configurations considered (LBE MM-ALE)

All Air Configurations

Tracer	Distance From Edge of Receptor Layer (mm)
1	0
2	50
3	100
4	200
5	300
6	400

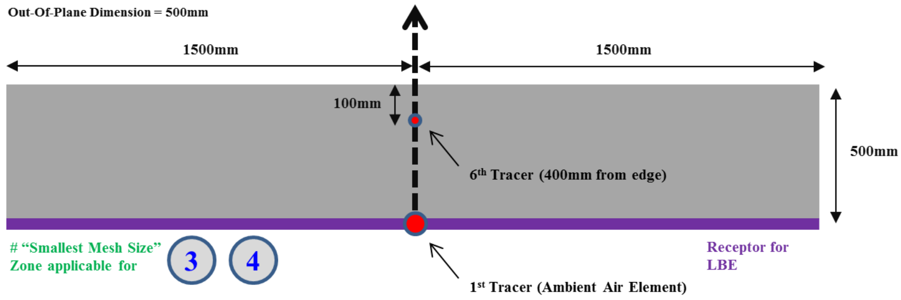

Figure 3: Location of Tracers & Smallest Mesh Size Zone (LBE MM-ALE)

All four air configurations were subjected to blast at two different scaled distances, Z = 1.5 ft/lb$^{1/3}$ and Z = 4 ft/lb$^{1/3}$, representing "impulsive" and "pressure" loading regimes respectively. The two scaled distances were chosen based on UFC 3-340-02 and ASCE Standard 59-11 [8]. Both standards have defined Z < 3.0 ft/lb$^{1/3}$ as close-in range while the opposite is for far-field range.

It is worthwhile to note the major difference between the two loading regimes. In blast engineering, an "impulsive" loading regime happens at a short stand-off distance, while a "pressure" loading regime is with respect to a far stand-off distance. There is an intermediate region, which is sometimes known as the "dynamic" loading regime. More importantly from a design point of view, the kinetic energy imparted to the structure in the "impulsive" loading regime is the governing criterion rather than the work done, and the opposite is true for "dynamic" loading regime". In fact, analytical methodologies such as Single-Degree-Of-Freedom (SDOF) and Multi-Degree-Of-Freedom (MDOF) are based on this principle.

Figures 4a, 4b & 4c display the simulation results for all four air configurations with regards to the two scaled distances, Z = 1.5 ft/lb$^{1/3}$ and Z = 4 ft/lb$^{1/3}$. The analytical solutions were based on utilizing the LBE keyword on a simple arbitrary Lagrangian problem for direct derivation of the pressure time histories due to empirical blast models.

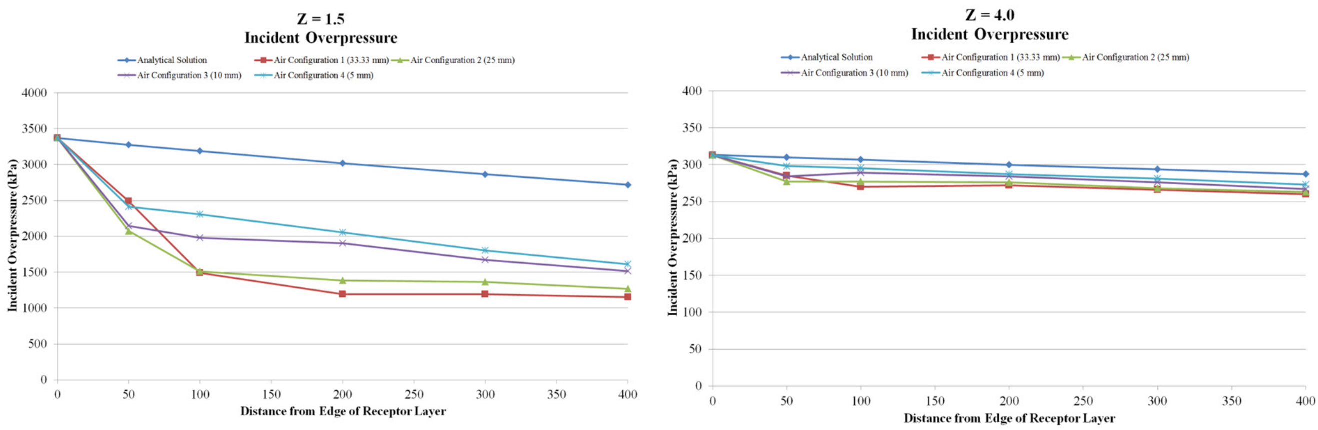

Figure 4a: Incident Overpressure (Z = 1.5 versus Z = 4.0)

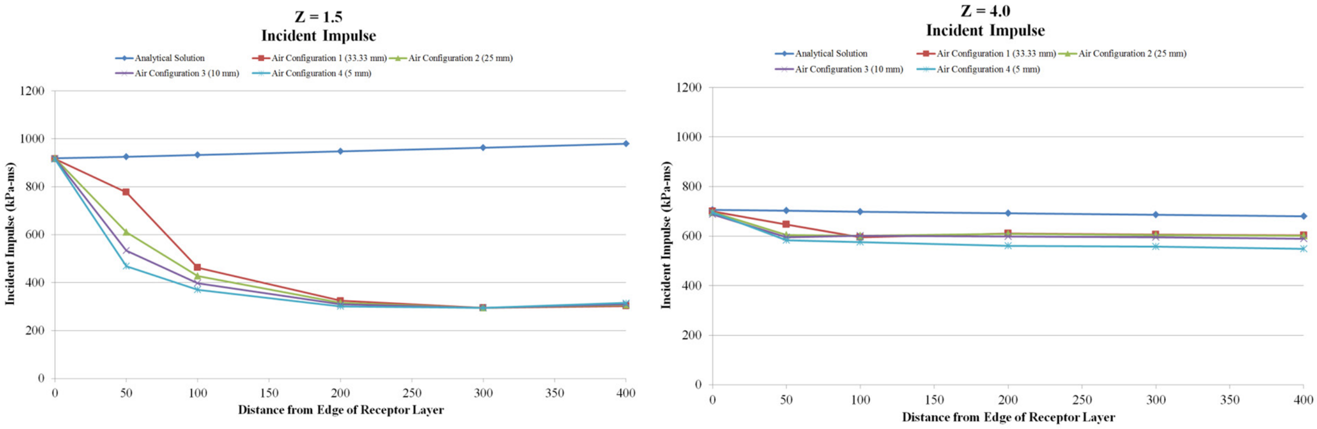

Figure 4b: Incident Impulse (Z = 1.5 versus Z = 4.0)

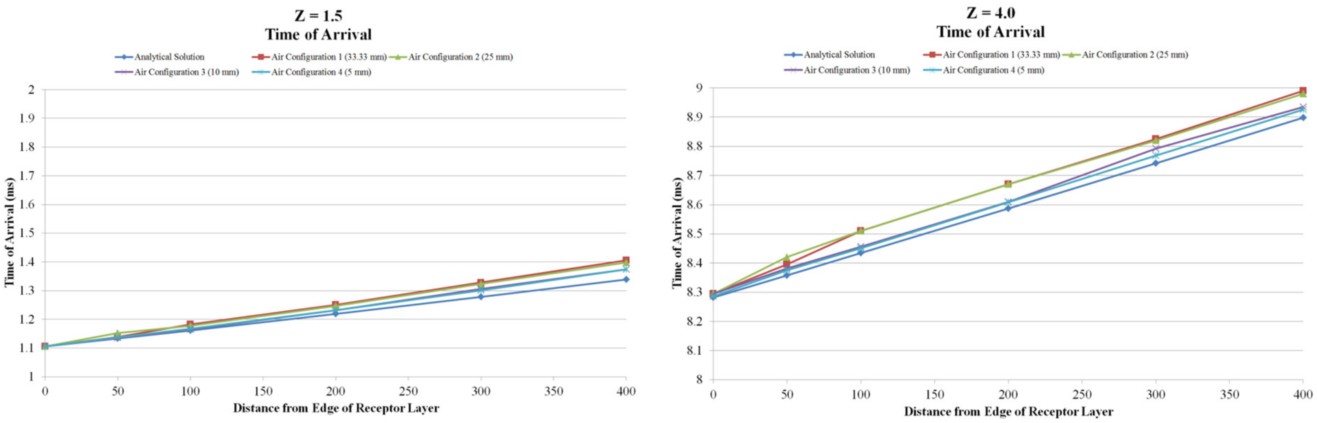

Figure 4c: Time of Arrival (Z = 1.5 versus Z = 4.0)

For Z = 1.5 ft/lb$^{1/3}$, it is apparent that all four configurations were not able to match analytical solutions in terms of both incident overpressure and impulse. Once beyond the first immediate air element behind the receptor layer, sharp decreases for both incident overpressure and impulse were observed. The readings for incident overpressure recorded up to 61 % difference while that for impulse scored up to 70 % difference as compared to analytical solutions. It is of interest to note that the percentage difference for incident overpressure calculations reduced from Air Configuration 1 to 4, i.e. as the immediate region of blast propagation became finer in terms of mesh size, while that for impulse stayed stagnant across all four configurations. The time of arrival in all four configurations provided reasonable comparisons to analytical solutions, accounting for up to only 1 % difference.

For Z = 4.0 ft/lb$^{1/3}$, in contrast, it appears that all quantities, i.e. incident overpressure, impulse and time of arrival, had better correlation to analytical solutions. The maximum percentage differences in incident overpressure and impulse were 12 % and 20 % respectively while that for time of arrival was also at a maximum of 1 %. The same trend could be observed for the percentage difference for incident overpressure calculations. Values matched closer as the immediate region of blast propagation became finer in terms of mesh size. However, impulse readings showed no distinct pattern.

The overall finding that all four configurations appeared invariant with respect to scaled distance, Z = 1.5 ft/lb$^{1/3}$, may be due to the way the LBE coupling is being defined rather than the boundaries' effects or the mesh size in the immediate region of blast propagation. . This observation may have reinforced the point raised in [3] that the fluid (air) velocity prescribed at the boundary for LBE coupling is approximate.

From a design point of view, codes such as ASCE Standard 59-11 generally allow advanced non-linear finite element analyses for close-in scenarios, because these situations involve complex structural response modes beyond what simplified methods such as Pressure-Impulse (PI) charts, SDOF and/or MDOF can handle, and blast propagation for close-in range is highly non-uniform. This is therefore an area of concern as the LBE MM-ALE coupling method will result in under-prediction of impulse, and consequently, under-prediction of the structural response due to the lack of resolution on fluid (air) velocity.

3. FSI

Good FSI calculations have to go hand in hand with accurate air blast propagation calculations in order to ensure that the correct loadings are imparted to the structure from the air. The need to check for integrity of FSI computations is emphasized in numerous documents, such as the section on *Constrained_Lagrange_in_Solid (CLIS) in Keyword Manual [1], a publication by LSTC [9] that offers detailed step-by-step guidelines and also good practices with regards to use of CLIS for FSI. The common underlying concept is first to track fluid movement and be able to visualize if leakage happens, before applying techniques to counter leakage, for example, by defining the coupling stiffness in the form of a curve (via parameter PFAC in CLIS) just enough to avoid leakage. If excessive leakage still persists, one can intervene by turning on leakage control (via parameter ILEAK in CLIS) while making sure that the leakage control forces are small compared to main penalty coupling forces.

One question is therefore whether the recommended treatment applies to solid elements. For a structure made up of shell elements, it is possible to have clearly defined fluid interfaces interacting with a Lagrangian surface to the extent of having two separate sets of ALE Multi-Material Group (AMMG), one on either side of the structure. The same cannot be done for a structure made up of solid elements as there is no fluid in the structure physically.

A series of arbitrary models were created with a pseudo fluid having the properties of air within the structure to allow demarcation of AMMGs and coupling was applied only to the "air outside". Consistently across the models, leakage was observed almost instantly, as seen from Figure 5. It was established that no amount of modification via PFAC and ILEAK could help.

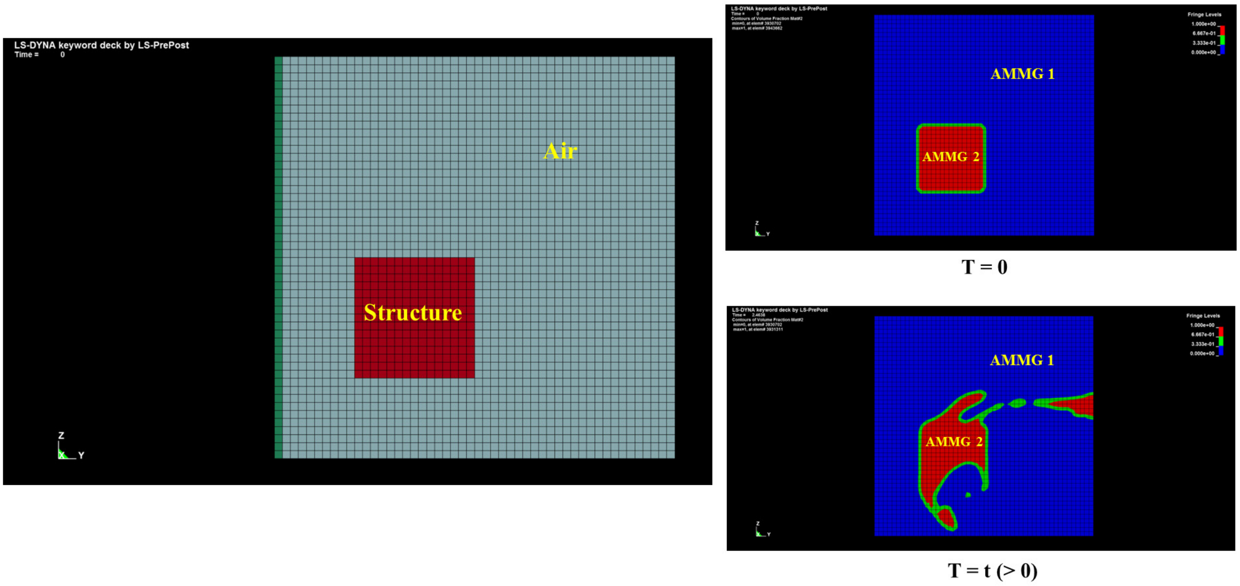

Figure 5: Illustration of Leakage (Couple to "Air Outside" only)

After concluding that coupling only to the "air outside" could not work, further trials were done to investigate the effects of coupling to both "air outside" and "air inside", on account that the only way to visualize leakage is by having more than one AMMG.

Table 1 reports the four combinations in which three key inputs were selected for modification in order to test how double AMMG couplings work for solid elements. For each combination, three coupling slave types were explored: "by Part", "6 Segments" and "by Segment Set". All structural solid and air elements were of regular mesh size of 20 mm. *DATABASE_FSI keyword was used to track the average coupling pressure on all six sides of the structure. As a reference, "Couple by Part in a single AMMG" was also conducted.

Figure 6 illustrates the typical volume fraction plots with respect to the four combinations. They were vastly different from cases that had considered coupling only to the "air outside". Just by defining coupling stiffness brought about the most significant improvement on leakage.

Figure 7 plots the average coupling pressure of the front segment directly facing the blast source for all cases. It was noted that the results from "6 Segments" combination were slightly different from the rest, recording 15 % higher peak pressure.

	Without PFAC Curve	PFAC Curve + No Leak	PFAC Curve + Leak	PFAC Curve + 2 Leaks
A	PFAC = 0.1	7, 14 or 21 MPa to modify coupling stiffness	7, 14 or 21 MPa to modify coupling stiffness	7, 14 or 21 MPa to modify coupling stiffness
B	Off	Off	On	On
C	Off	Off	Off	On

```
*CONSTRAINED_LAGRANGE_IN_SOLID
$#   slave    master     sstyp     mstyp     nquad     ctype     direc     mcoup
         1         1         1  A      0         4         4         2        -1
$#   start       end      pfac      fric    frcmin      norm   normtyp      damp
    0.0001.0000E+10  0.100000     0.000  0.500000         0         0     0.000
$#      cq      hmin      hmax     ileak     pleak   lcidpor     nvent  blockage
     0.000     0.000     0.000         0  0.100000         0         0         0
$#  iboxid   ipenchk   intforc   ialesof B  lagmul    pfacmm      thkf
         0         1         1         0     0.000         0     0.000
*CONSTRAINED_LAGRANGE_IN_SOLID
$#   slave    master     sstyp     mstyp     nquad     ctype     direc     mcoup
         1         1         1         0         4         4         2        -2
$#   start       end      pfac      fric    frcmin      norm   normtyp      damp
    0.0001.0000E+10  0.100000 C   0.000  0.500000         1         0     0.000
$#      cq      hmin      hmax     ileak     pleak   lcidpor     nvent  blockage
     0.000     0.000     0.000         0  0.100000         0         0         0
$#  iboxid   ipenchk   intforc   ialesof    lagmul    pfacmm      thkf
         0         1         1         0     0.000         0     0.000
```

Table 1: Four Combinations with Three Key Inputs for Modification

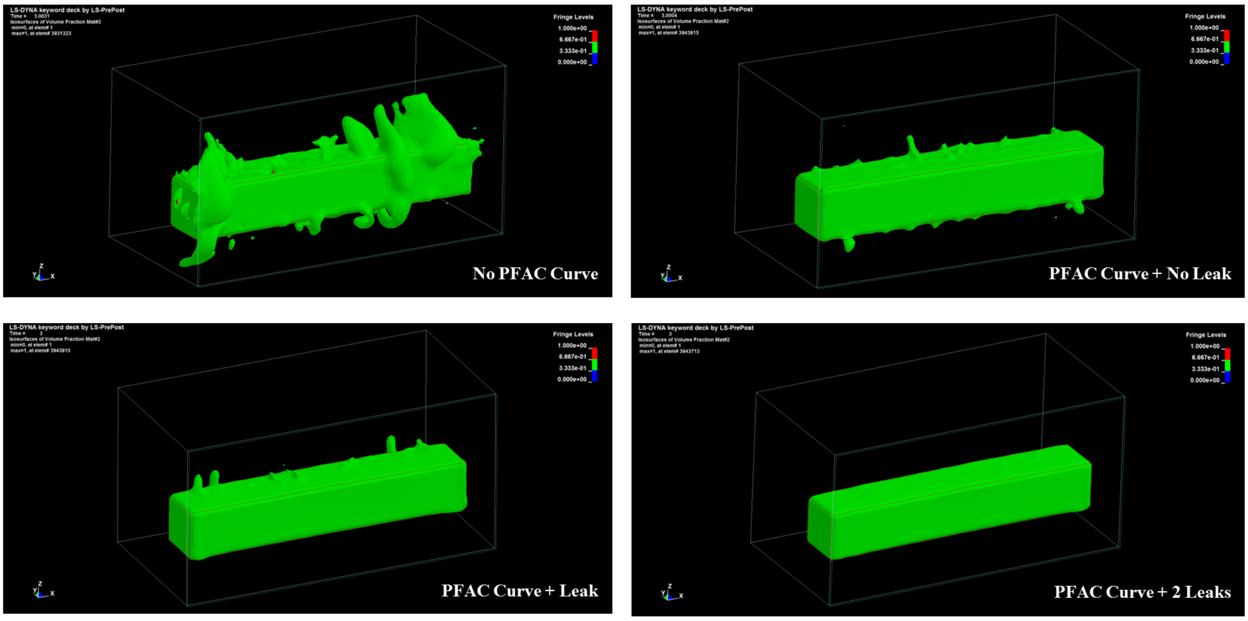

Figure 6: Typical Volume Fraction Plots of the Four Combinations

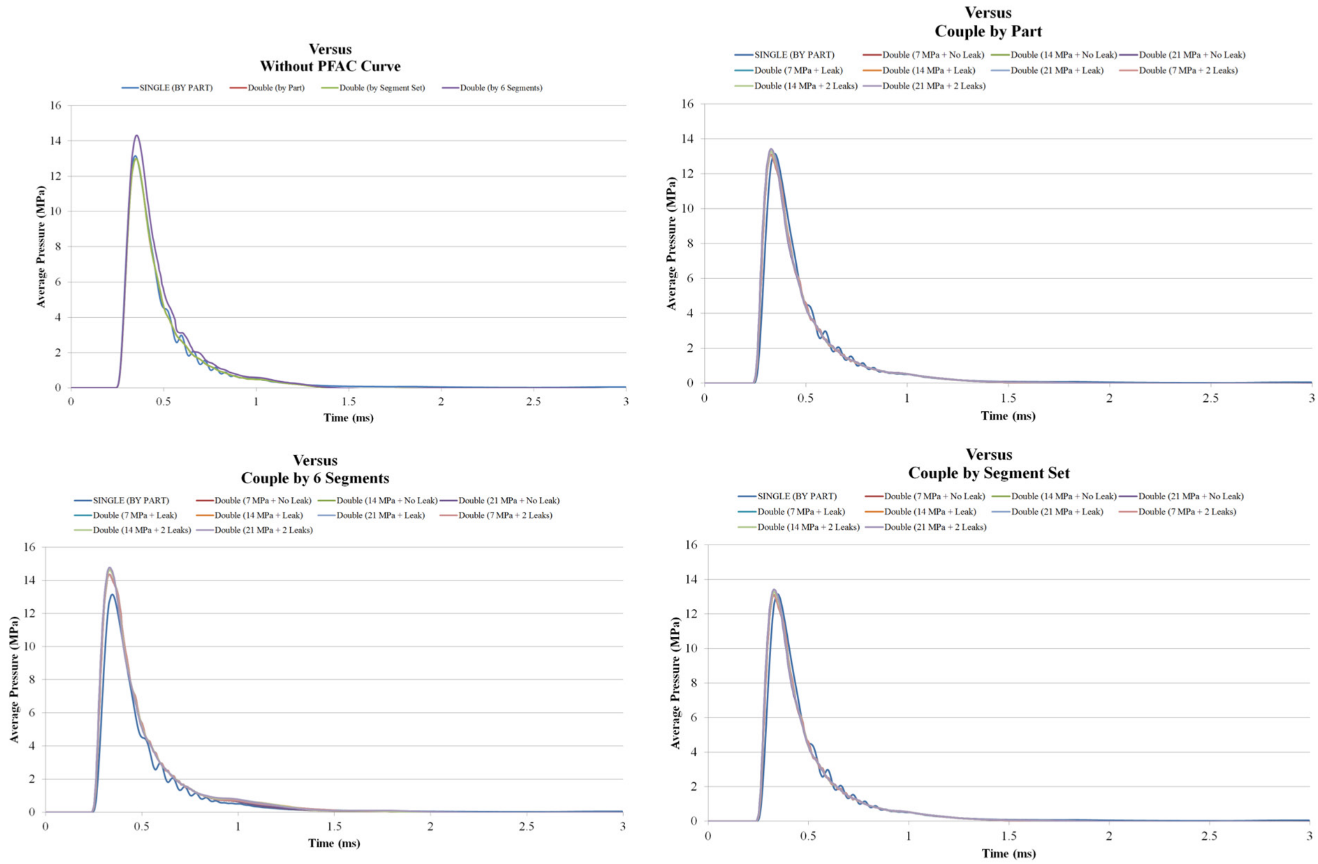

Figure 7: Average Coupling Pressure of Front Segment for All Cases

It is interesting to see that despite having two AMMGs, outside and inside the structure, the average coupling pressure on the front segment remained the same as that of the reference case, which is “Couple by Part in a single AMMG”. This was true across all cases, even though different coupling stiffness, leakage control and coupling slave types were used and varying levels of leakage were seen correspondingly. These findings suggest that the concept to visualize fluid interface so as to track and prevent leakage is unique only to shell elements and rightfully so, as it is physical to accommodate two separate sets of AMMG, one on either side of the structure. The concept is not exactly applicable for structures made up of solid elements as these series of test runs had proven that the structural response would be independent regardless of what one modifies.

One of the possible alternatives of checking integrity of FSI computations for structures made up of solid elements can be by comparing the coupling pressure on the surfaces against known solutions wherever possible. Another method can be by making sure that air blast propagation calculations are accurate from the source leading up to the target through mesh convergence studies. Without correct incident pressure time histories, it is unlikely that the corresponding reflected quantities would be accurate.

4. Case-Study

Figure 8 shows the LBE MM-ALE FSI model created for the case-study. With reference to [4], only one (out of the four cases) was considered, i.e. *MAT_159 @ Scenario 1. Details about the element formulations, material properties, contact keywords, hourglass controls etc. involved in various components of the structure can also be found in [4]. The concrete portion of the steel-jacketed beam-column was coupled by part to air block (as a single AMMG) made up by regular mesh sizes of 33.33 mm.

Based on the findings gathered from prior studies on LBE MM-ALE coupling method, it was expected that the resulting blast loadings would be under-estimated independent of the mesh size employed. The corresponding structural response would also not match pre-test computations using the CFD-Lagrangian approach which compared well with experimental data. Therefore, since the intention behind the case-study was to demonstrate the extent of deviation due the LBE MM-ALE coupling method rather than to aim for close correlations, the following two aspects were further approximated. First, instead of creating a ground surface in the model for interaction with blast propagation due to empirical spherical air burst, the empirical hemispherical surface burst was considered. The Mach Stem feature did not seem to be valid for close-in cases at low height of detonation, as evident from the onscreen warning messages. Second, no axial preload of the beam-column was included. In-built compression is known to enhance shear strength of a beam-column which in turn improves its flexural capacity, and hence the omission would lead to conservative results.

Figure 9 compares the mid-span displacement profiles and the post-blast residual axial capacities for both CFD-Lagrangian approach and LBE MM-ALE coupling method. Table 2 and 3 summarize the simulation results obtained against experimental data. It was noted that the impulse at mid-span by LBE MM-ALE coupling method was only 38 % of field measurement while the post-blast axial capacity was 15 % higher.

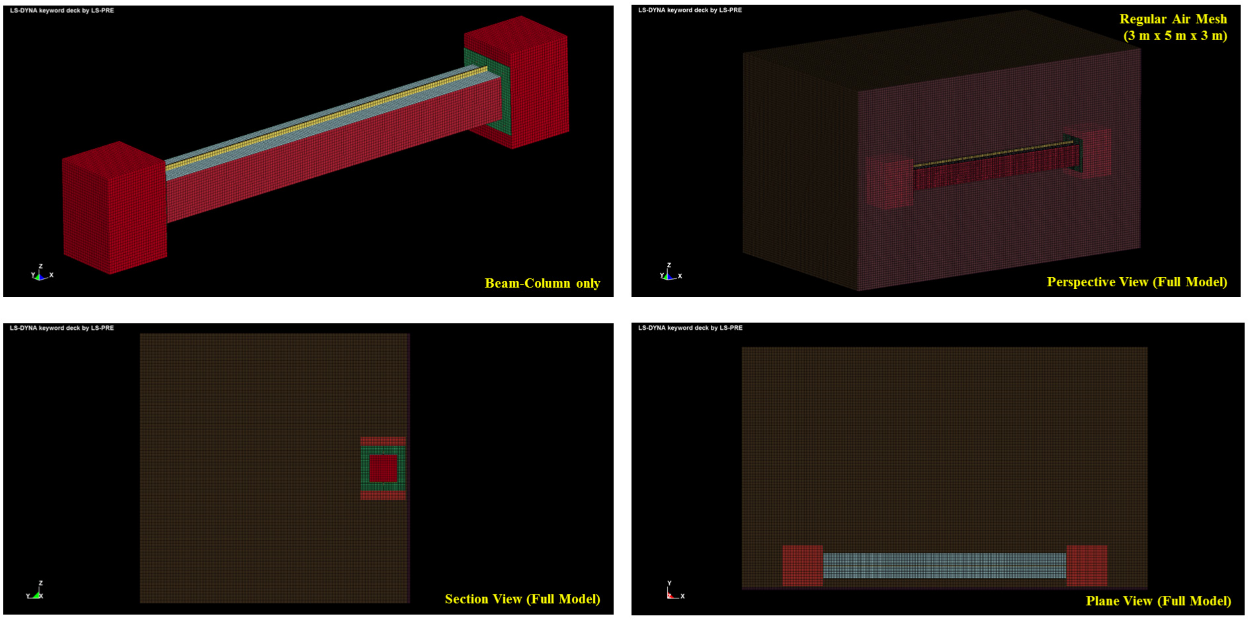

Figure 8: LBE MM-ALE FSI Model (Case-Study)

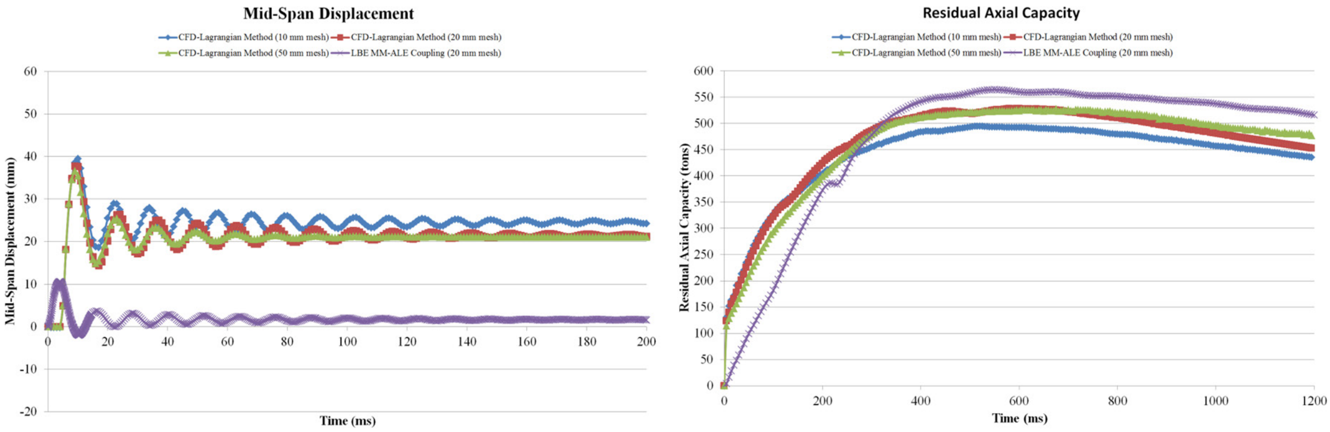

Figure 9: Mid-Span Displacement & Residual Axial Capacity Simulation Results

	Impulse at Mid-Span (kPa-ms)						
	I_{100}	I_{75}	I_{50}	$I_{Extrapolated}$	p	$GCI_{50/75}$	95% Confidence Interval
CFD	10607	10756	11312	11736	2.066	0.04687	[10781 , 11842]
			Measured	12914			

	Via *DATABASE_FSI	
LBE MM-ALE	**4803**	kPa-ms

Table 2: Impulse (by LBE MM-ALE) versus CFD and Field Measurement

	Permanent Mid-Span Deformation (mm)						
	X_{50}	X_{20}	X_{10}	$X_{Extrapolated}$	p	$GCI_{10/20}$	95% Confidence Interval
CFD-Lagrangian Method	21.05	21.24	24.21	24.26	5.9358	0.003	[24.15 , 24.27]
LBE MM-ALE Coupling	-	**1.57**	-	-	-	-	-
			Measured	54			

	Residual Axial Capacity (tons)						
	R_{50}	R_{20}	R_{10}	$R_{Extrapolated}$	p	$GCI_{10/20}$	95% Confidence Interval
CFD-Lagrangian Method	527.00	528.10	494.77	494.54	7.248	0.00056	[494.49 , 495.04]
LBE MM-ALE Coupling	-	**564.30**	-	-	-	-	-
			Measured	493.8			

Table 3: Permanent Mid-Span Deformation & Residual Axial Capacity (by LBE MM-ALE) versus CFD-Lagrangian and Field Measurement

5. Conclusions

This paper shared the experiences gathered on separate studies conducted on LBE MM-ALE and FSI and presented a case-study in which results from the LBE MM-ALE FSI simulation were compared to the results from earlier pre-test computations using the CFD-Lagrangian approach and associated field measurements.

The validity of LBE MM-ALE coupling method to handle analyses involving structures against close-in detonation effects is an area of concern, as the lack of resolution on fluid velocity will result in under-prediction of impulse. The integrity of FSI computations for structures made up of solid elements has to be checked by alternative approaches, either by comparing the coupling pressures against known solutions wherever possible, or by mesh convergence studies to ensure air blast propagation is calculated correctly from the source leading up to the target.

6. References

[1] LS-DYNA 971 R6.1.0 Keyword Manuals I & II, 2012
[2] Slavik, T. "A Coupling of Empirical Explosive Blast Loads to ALE Air Domains in LS-DYNA", 7th European LS-DYNA Users Conference, 2009
[3] Len Schwer. "A Brief Introduction to Coupling Load Blast Enhanced with Multi-Material ALE: The Best of Both Worlds for Air Blast Simulation", German LS-DYNA Forum, 2010
[4] Swee Hong Tan, Jiing Koon Poon, Roger Chan, David Chng. "Retrofitting of Reinforced Concrete Beam-Column via Steel Jackets against Close-in Detonation", 12th International LS-DYNA Users Conference, 2012
[5] ASME V&V 10-2006. Guide for Verification and Validation in Computational Solid Mechanics
[6] ASME V&V 20-2009. Standard for Verification and Validation in Computational Fluid Dynamics and Heat Transfer
[7] UFC 3-340-02 (5 December 2008). Unified Facilities Criteria (UFC): Structures to Resist the Effects of Accidental Explosions
[8] ASCE Standard 59-11. Blast Protection of Buildings, 2011
[9] Guidelines for ALE Modeling in LS-DYNA, 2009